Appl Phys A (2010) 101: 487–490
DOI 10.1007/s00339-010-5885-8

Applied Physics A
Materials Science & Processing

Enhanced machining of steel using femtosecond pulse pairs

Carl M. Liebig · P. Srisungsitthisunti · A.M. Weiner · X. Xu

Received: 31 October 2009 / Accepted: 24 May 2010 / Published online: 3 July 2010

Abstract In this study we report on the ablation of steel using femtosecond double-pulse trains. Double-pulse trains with pulse-to-pulse separations between 1 ps and 1 ns were used to machine micro-channels in a steel sample. The depths of the laser-ablated channels were measured to characterize the efficiency of the ablation process. Results show that using a double-pulse train with an optimal separation time dramatically increases the ablation depth and does not deposit unwanted material that may require additional post-processing of the machined surface.

1 Introduction

The process of laser micromachining has been well developed. Although using nanosecond laser pulses is common for micromachining in many materials, high thermal conductivity has limited the efficiency in machining metals due to damage beyond the desired area [1]. Machining with laser pulses with femtosecond pulsewidths has been shown to limit the amount of thermal diffusion due to the very short heating duration, and also due to a rapid solid-to-vapor phase transition, limiting the absorption region to the penetration of the optical pulse thus limiting the collateral damage [2]. When using nanosecond pulsewidths for ablation, the ejected material is often deposited outside of the ablated region; this process often requires post-processing in order to remove the debris [3]. The non-thermal nature of ablation with femtosecond pulses, mostly for dielectric materials, has shown that these complications can be avoided [4].

Temporal shaping of femtosecond pulses has allowed the customization of how the optical energy is deposited in many materials [5]. Stoian et al. has shown that by using multi-pulse femtosecond pulse trains it is possible to optimize the ablation process in several large band-gap dielectric materials. A decrease in damage to areas outside of the ablated region and an increase to the ablated depth is due to the initial pulses "preparing" the electronic and thermal properties of the surface of the material for ablation by the subsequent pulses [6]. Although the ultrafast ablation pathways differ between dielectrics and metals, there is evidence that multi-pulse trains have facilitated the machining process when there are nanosecond time delays between both picosecond and nanosecond pulses [7, 8]. In these cases the second pulse interacts with the thermal effects of the ablation process and not the non-thermal processes that occur due to ultrafast excitation. In this work we investigate the use of femtosecond double-pulse trains to optimize the machining of metal (steel). Femtosecond double-pulse trains at several fluences were generated with pulse-to-pulse separation from 1 ps to 1 ns, and used to machine channels in steel plates. The depth of the channels machined in steel plates as well as the surface topography was characterized in order to determine the optimal pulse spacing for machining steel.

2 Experimental setup

Figure 1 shows a schematic of the experimental setup used in this work to machine steel samples. A Spectra Physics Spitfire regenerative amplifier producing 800 nm, 50 fs

C.M. Liebig · P. Srisungsitthisunti · X. Xu (✉)
School of Mechanical Engineering and Birck Nanotechnology Center, Purdue University, West Lafayette, IN 47907, USA
e-mail: xxu@ecn.purdue.edu

A.M. Weiner
School of Electrical and Computer Engineering, Purdue University, West Lafayette, IN 47907, USA
Fax: +1-765-494-0539

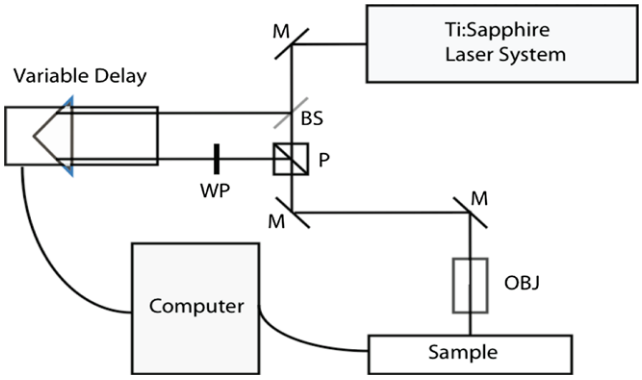

Fig. 1 Experimental setup used for the ablation of steel using femtosecond double-pulse trains. In diagram M corresponds to mirrors, WP to a 1/2-wave plate, P to a polarizing beam splitter, OBJ to a 10× objective

(FWHM) pulses at a repetition rate of 1 kHz with pulse energy up to ∼ 1 mJ was used. The pulses were divided by amplitude and traveled separate paths. One of the beam polarizations was rotated 90 degrees using a $\frac{1}{2}$-wave plate. The beams were then spatially overlapped using a polarizing beam splitter. This configuration allows the intensity of the overlapped beams to be independently controlled using separate $\frac{1}{2}$-wave plate and polarizer combinations. The pulses were temporally synchronized using a long travel translation stage, which was confirmed using cross-correlation. The long travel stage also allows time delays of greater than one nanosecond between the pulses. The overlapped pulses were then focused using a 10× objective onto the steel sample, which was mounted on a 3-dimensional high precision translation stage, allowing for smooth and accurate movement of the sample for machining.

For all the experiments the intensities of the two pulses were equal. The estimated diameter of the focused beam was 20 μm. The total incident fluences used were 16.7 J/cm^2, 13.7 J/cm^2, 8.7 J/cm^2 and 5.0 J/cm^2. The incident beam was controlled using a computer-interfaced shutter synchronized with the translation stages. The machined area was created using double-pulse delays that vary from 1 ps to 1 ns, by translating the sample at a speed of 20 μm/s for creating a 200 μm-long channel. Single femtosecond pulses with the same total energy of the pulse pair were also used as a comparison. There was no measurable difference between each polarizations used for the single pulse measurements, therefore no polarization effects are expected for the cross-polarization used in the double-pulse ablation. Each measurement was repeated 5 times in order to improve the accuracy of the depth measurements of the machined areas.

To determine the effect of the pulse separation on the machining efficiency, a measurement of the profile of the machined area was necessary. The topography of the laser-machined channels was analyzed using a surface profiler (Alpha-Step IQ). Each of the laser-ablated channels was

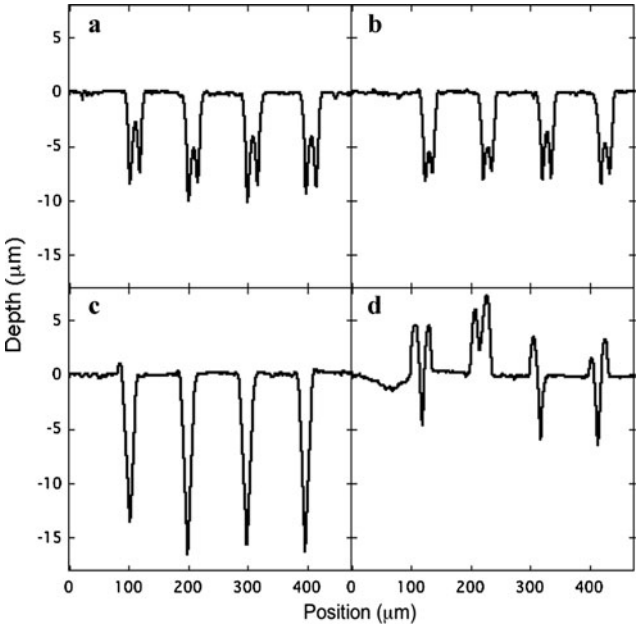

Fig. 2 Surface profile of steel sample after ablation with ∼1000 femtosecond at a fluence of 13.7 J/cm^2 with (**a**) single pulses and double-pulse trains with delay times of (**b**) 1 ps, (**c**) 10 ps, and (**d**) 1 ns

measured two times to account for variation in the surface of sample. The laser-ablated regions were also examined with an SEM (Hitachi S-4800 FESEM) in order to aid in the visualization of the laser-machined channel.

3 Results and discussion

A comparison between the channels machined in steel using femtosecond pulse pairs with variable pulse separation shows that there is a difference in the ablated material as well as the material that is deposited outside of the laser impact zone. Figure 2 shows four plots of the surface profile of the laser-ablated regions, for single pulse and pulse pairs with separations of 1 ps, 10 ps, and 1 ns for a total fluence of 13.7 J/cm^2. These results can be directly compared with SEM micrographs in shown in Fig. 3. Experiments with many other pulse separation times were performed and were not presented here due to space limitation, but are summarized in Fig. 4. With the sample travel speed of 20 μm/s and the laser focused spot size of 20 μm, approximately 1000 pulses were incident on any point in the middle section of the channel. In Fig. 2(a) through (c) it was observed that for single pulses and for double pulses with 10 ps of less delay between pulses, there was little splashed liquid corona measured which appears as ridges outside of the machined channel. The depth of the channel is about 8 μm for single pulse ablation and remains similar for 1 ps delay. However, there are significant differences that occur within the ablated

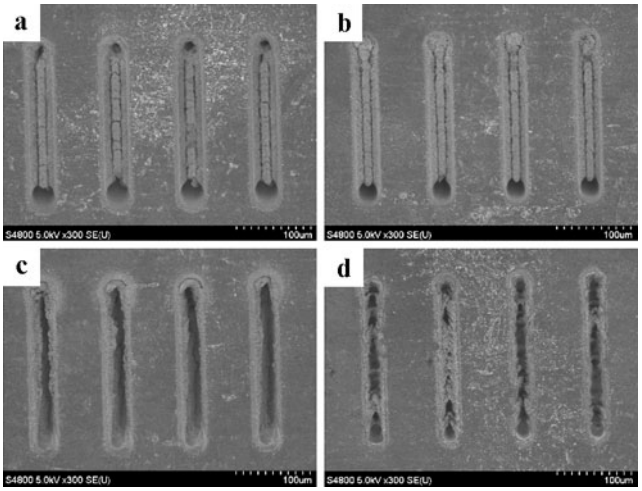

Fig. 3 SEM images of steel sample after ablation with ~1000 femtosecond at a fluence of 13.7 J/cm^2 with (**a**) single pulses and double-pulse trains with delay times of (**b**) 1 ps, (**c**) 10 ps, and (**d**) 1 ns

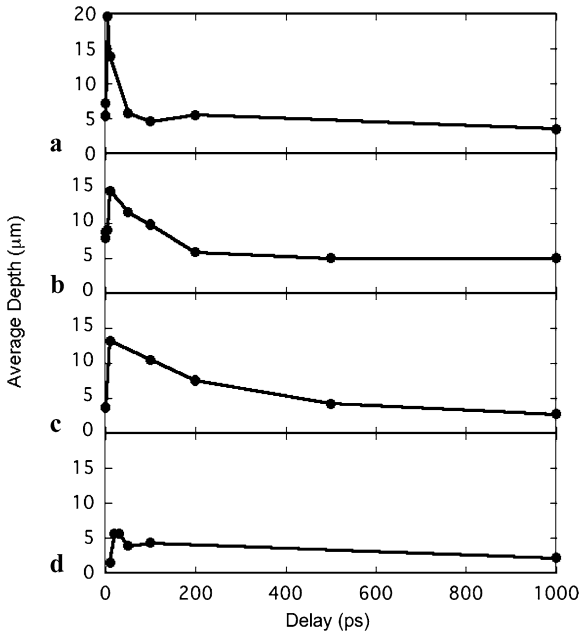

Fig. 4 Average depth of laser-ablated channel with delays between 0 and 1 ns for fluences of (**a**) 16.7 J/cm^2, (**b**) 13.7 J/cm^2, (**c**) 8.7 J/cm^2 and (**d**) 5.0 J/cm^2

channel that may play a role in the efficiency of the machining process.

For the single pulse excitation and double-pulse excitation with 1 ps separation time, similar results were observed to due to the pulse separation being less than the expected electron–phonon coupling time. There is a large central peak or ridge within the laser-machined channel. When the pulse separation is less than the electron–phonon coupling time both pulses interact with the material before melting can occur. This central peak is observed in some cases to even exceed the depth of the channel. The central peak reduces the quality of the machined channel and reduces the efficiency of machining. The SEM micrographs in Figs. 3(a) and (b) show the images of the central ridges. The central ridge could be composed of re-solidified material that was unable to escape the machined channel during the ablation process as the sample is being translated. The material that is unable to be ejected from the ablated region builds up and reduces the machining depth of the channel. Similarly shaped features have been observed previously for femtosecond ablation of metals, where a bump was formed at the center of the machined surface [9]. This feature can be caused by surface-tension-driven-flow of the molten layer [10]. After the laser pulse radiates and ablates the surfaced, there is a molten layer, which initially flows outward from the center but then reverses the flow direction and flows inward, which may cause the central ridge.

A different behavior was observed when a pulse delay between 5 ps and 10 ps was used for ablation. For 5 ps delay there was a decrease in the height of the central peak, but was still visible from the measurements. The average depth of channel increases to 9 μm. At 10 ps delay time, shown in Fig. 2(c), there is a significant difference in the profile of the ablated region. Figure 3(c) shows an SEM image of the ablated region. It can be seen that there is no visible ridge in the laser-ablated channel. The average depth of the central channel was measured to be 14.6 μm. The change in the behavior of the central peak indicates a change in the surface of the target material 5 to 10 ps after the pulse excitation. Calculations using a combination of the two-temperature model and molecular dynamics (MD) simulation show that when aluminum, copper and nickel are excited with a single ultrafast pulse there is a separation of the ablated material from the residual liquid region that occurs between 5 and 10 ps after excitation [11–14].

If steel behaves similarly, as all other metals we have studied (the potential function for steel needed for MD calculations is not readily available), the second pulse reaches the sample and interacts with the material as the ablated material is separating itself from the bulk. This changes the ablation process, and will eventually change the temperature field and the molten liquid flow pattern that could be the cause of the formation of the central ridge.

Reheating of the ejected plasma has been shown to have an effect on the ablation process when double-pulse have been used for ablation of metals. Recent studies show a decrease in the ablation rate when double pulses with separations longer than the electron–phonon coupling time are used for ablation in several metals [15–17]. Our measurements appear to be different from these studies as the exact delay time for achieving the maximum depth obtained in our study is different. However, the exact time delay to achieve maximum ablation depth depends on the complex dynamics

after laser pulse irradiation, such as plasma shielding and melting formation, which not only depend on materials but also fluence. Adding to the complexity of this study is that the sample is being translated during ablation, which can influence the ablation depth as the second laser pulse can move some of the melted materials into the previously ablated area, and reduce the ablation depth, resulting in lower machining efficiency compared with some of the previously reported results. The prediction on the ablation depth vs. time requires comprehensive numerical modeling, which is beyond the scope of this work.

For pulse separation times longer than 10 ps, the topography of the laser-ablated area changes once again. At a 20 ps delay between pulses, ridges surrounding the laser-ablated region begin to appear. The depth of the ablated channel begins to decrease. This trend was measured for all delays between 20 ps and 1 ns, the longest time delay used in this experiment. The decrease in the ablation depth and the development of the ridges that occurs between 20 ps and 1 ns may indicate a decreased interaction with the ablated material and an increased interaction with the remnant liquid layer. Figure 2(d) shows the profile of the laser-ablated channels with a delay of 1 ns. SEM images of the ablated region are shown in Fig. 3(d). Evidently, the ridges outside the channel are caused by "splashing" of the molten material by the second pulse. This may be a sign of interaction of the second pulse with the high temperature liquid layer. Similar ridges have also been observed for ablation using nanosecond pulses and the splashing is purely a thermal process [2]. In addition to visible ridges surrounding the channel, there are also large particulates in the channel itself that may be caused by liquid material that does not escape the channel before cooling. The SEM images also show less consistency among the four channels, indicating the splashing process is quite random.

Figure 4 shows the average depth of the laser-ablated channel as a function of the delay between the pulses for fluences (a) 16.7 J/cm^2, (b) 13.7 J/cm^2, (c) 8.7 J/cm^2, and (d) 5.0 J/cm^2. It can be seen that for 13.7 J/cm^2 the ablation depth reaches a maximum value when the delay between the pulses is $\sim$10 ps. The pulse-to-pulse delay for obtaining the maximum depth is about $\sim$5 ps when the fluence is 16.7 J/cm^2, and is longer, $\sim$30 ps for the low laser fluence of 5.0 J/cm^2. Topographically for all of the fluences the ablation phenomena are similar although the features are attenuated at lower fluences: at long delays between pulses there is an increased ridge outside of the ablated channels due to the second pulse interacting with the liquid layer; for pulse separations less than the optimum delays, a central peak developed within the ablated channel. Therefore, by making simple adjustments to the separation times of the pulses, we are able to take advantage of the ultrafast ablation dynamics and increase the efficiency of machining.

4 Conclusions

We have shown that using femtosecond pulse pairs can improve machining. By using femtosecond double pulses and varying the delay between pulses, the results of machining of steel have been explored. Not only does adjusting the separation between the double pulses allow for the elimination of the central ridges that exist in the channels machined using single pulses, we have also shown that a temporal window exists for delays between the pulses, for which the depth of the machined channel is greatly increased compared to single pulses. Furthermore, increasing the separation time results in splashing of the molten liquid, similar to what happens in longer pulse machining, and a decrease in machining depth.

Acknowledgements Support to this project by AFOSR STTR, Contract No. FA8650-09-M-2971 is gratefully acknowledged. The authors also thank Mr. James I. Mitchell for taking the SEM images.

References

1. C. Momma, S. Nolte, B.N. Chichkov, F. von Alvensleben, A. Tünnermann, Appl. Surf. Sci. **109/110**, 15 (1997)
2. J. Yang, Y. Zhao, X. Zhua, Appl. Phys. Lett. **88**, 094101 (2006)
3. M.D. Perry, B.C. Stuart, P.S. Banks, M.D. Feit, V. Yanovsky, A.M. Rubenchik, J. Appl. Phys. **85**, 6803 (1999)
4. G. Dumitru, V. Romano, H.P. Weber, M. Sentis, J. Hermann, S. Bruneau, W. Marine, H. Haefke, Y. Gerbig, Appl. Surf. Sci. **208/209**, 181 (2003)
5. R.S. Judson, H. Rabitz, Phys. Rev. Lett. **68**, 1500 (1992)
6. R. Stoian, M. Boyle, A. Thoss, A. Rosenfeld, G. Korn, I.V. Hertel, E.E.B. Campbell, Appl. Phys. Lett. **80**, 353 (2002)
7. M. Lapczyna, K.P. Chen, P.R. Herman, H.W. Tan, R.S. Marjoribanks, Appl. Phys. A **69**, S883 (1999)
8. A.C. Forsman, P.S. Banks, M.D. Perry, E.M. Campbell, A.L. Dodell, M.S. Armas, J. Appl. Phys. **98**, 033302 (2005)
9. J. Koch, F. Korte, T. Bauer, C. Fallnich, A. Ostendorf, B.N. Chichkov, Appl. Phys. A **81**, 325 (2005)
10. D.A. Willis, X. Xu, ASME J. Heat Transf. **122**, 763 (2000)
11. S. Sonntag, J. Roth, F. Gaehler, H.-R. Trebin, Appl. Surf. Sci. **255**, 9742 (2009)
12. C. Cheng, X. Xu, Appl. Phys. A **79**, 761 (2004)
13. X. Xu, C. Cheng, I.H. Chowdhury, ASME J. Heat Transf. **126**, 727 (2004)
14. C. Cheng, X. Xu, Phys. Rev. B **72**, 165415 (2005)
15. A. Semerok, C. Dutouquet, Thin Solid Films **453–454**, 501 (2004)
16. T. Donnelly, J.G. Lunney, S. Amoruso, R. Bruzzese, X. Wang, X. Ni, J. Appl. Phys. **106**, 013304 (2009)
17. M.E. Povarnitsyn, T.E. Itina, K.V. Khishchenko, P.R. Levashov, Phys. Rev. Lett. **103**, 195002 (2009)